Matrix Gla Protein Reinforces Angiogenic Resolution

Bikram Sharma[1] and **Allan R. Albig**[2]

[1]Department of Biology, Indiana State University, Terre Haute, IN 47809 USA

[2]Department of Biology, Boise State University, Boise ID. 83725

Abstract

Matrix Gla Protein (MGP) is an ECM molecule commonly associated with dysfunctions of large blood vessels such as arteriosclerosis and atherosclerosis. However, the exact role of MGP in the microvasculature is not clear. Utilizing a mouse MGP knockout model we found that MGP suppresses angiogenic sprouting from mouse aorta, restricts microvascular density in cardiac and skeletal muscle, and is an endogenous inhibitor of tumor angiogenesis. Similarly, morpholino based knockdown of MGP in zebrafish embryos caused a progressive loss of luminal structures in intersegmental vessels, a phenotype reminiscent of Dll4/Notch inhibition. Accordingly, MGP suppressed Notch-dependent Hes-1 promoter activity and expression of Jagged1 mRNA relative to Dll4 mRNA. However, inhibition of BMP but not Notch or VEGF signaling reversed the excessive angiogenic sprouting phenotype of MGP knockout aortic rings suggesting that MGP may normally suppress angiogenic sprouting by blocking BMP signaling. Collectively, these results suggest that MGP is a multi-functional inhibitor of normal and abnormal angiogenesis that may function by coordinating with both Notch and BMP signaling pathways.

Keywords

Angiogenesis; Extracellular Matrix; Matrix Gla Protein; Jagged-1; Delta Like 4; Notch Signaling; BMP signaling

Introduction

Angiogenesis is the development of new capillaries from pre-existing vessels. Normally, existing vasculature is stable and quiescent, held in stasis by a balance between pro- and anti-angiogenic molecules present in the vascular basement membrane and surrounding stroma. During angiogenesis, however, increasing pro-angiogenic stimuli present in the microenvironment upsets this balance and activates angiogenesis by binding to specific receptors present on endothelial cell surfaces. Upon activation, endothelial cells begin to loose their cell-to-cell adhesions, proliferate, dedifferentiate, and sprout toward the avascular

Corresponding Author Upon Submission: Allan R. Albig, PhD, Department of Biology, Science Bldg. Rm. 117, Boise State University, 1910 University Dr. Boise, ID 83725-1515 USA, AllanAlbig@boisestate.edu Phone: 208-426-1541.

Author Contributions:
BS and ARA conceptualized the study, performed experiments, analyzed data, and wrote manuscript.

Conflict of Interest:
Authors declare no conflict of interest.

Publisher's Disclaimer: This is a PDF file of an unedited manuscript that has been accepted for publication. As a service to our customers we are providing this early version of the manuscript. The manuscript will undergo copyediting, typesetting, and review of the resulting proof before it is published in its final citable form. Please note that during the production process errors may be discovered which could affect the content, and all legal disclaimers that apply to the journal pertain.

microenvironment. During the terminal phase of angiogenesis, endothelial cells re-differentiate, cease extraneous sprouting, organize themselves to form tubular structures, reconstitute a basement membrane, recruit mural cells (pericytes and vascular smooth muscle cells), re-establish cell-cell junctions, and return to cellular quiescence to form a stable vasculature (Carmeliet, 2000).

Inappropriate angiogenesis is involved in the pathogenesis of several diseases including cancer (Cao, 2009; Carmeliet and Jain, 2000; Dreyfus, 1989; Folkman, 2001). Therefore, therapeutic manipulation of angiogenesis represents an attractive approach for the treatment of these diseases. In order to improve angiogenic therapeutics however, the identification of both pro as well as anti-angiogenic molecules and characterization of their mechanism of action is important. Interestingly, extracellular matrix (ECM) not only provides a scaffold to the growing endothelial cells but also contains distinct angiogenic signals to initiate, drive, and complete angiogenic process (Davis and Camarillo, 1995; Davis and Senger, 2005). Indeed, several extracellular matrix (ECM) molecules have been identified as angiogenic regulators (Ingber, 1992; Sottile, 2004; Stupack and Cheresh, 2002; Stupack and Cheresh, 2003). Therefore, the complete characterization of ECM-based angiogenic molecules, and the molecular mechanism by which these molecules regulate angiogenesis represents an important, yet underdeveloped avenue towards potential angiogenic-based therapeutics.

Matrix Gla Protein (MGP) is an ECM molecule commonly found near vascular tissues (Hao et al., 2004; Luo et al., 1997; Yao et al., 2010). Primarily, MGP has been described as a calcification inhibitor and is crucial for the maintenance of normal vascular function (Luo et al., 1997; Yao et al., 2007). MGP –/– mice show severe aortic calcification and uniformly die within two months of birth (Luo et al., 1997). In addition, MGP polymorphisms have been linked to coronary artery calcification (Crosier et al., 2009; Herrmann et al., 2000), and MGP suppresses the formation of atherosclerotic lesions in the apolipoprotein E (APOE) knockout mouse model of human atherosclerosis (Yao et al., 2010). Mechanistically, MGP sequesters BMP2 and BMP4, thereby blocking BMP signaling through ALK receptors (Yao et al., 2006). However, it is not clear whether MGP suppresses vascular calcification via inhibition of BMP signaling alone or if additional mechanisms may be involved. In light of this, a recent discovery suggested that BMP alone is insufficient to promote smooth muscle calcification. Rather, BMP requires cooperation with the notch signaling pathway to promote vascular calcification (Shimizu et al., 2009; Shimizu et al., 2011). This observation is further supported by results showing that signaling through the BMP and Notch pathways synergistically suppress VEGF expression (Larrivee et al., 2012; Ricard et al., 2012).

MGP is not only physiologically important in large blood vessels, but also appears to be an important regulator of capillary function and angiogenesis. MGP suppresses excessive branching of pulmonary capillaries during vascular development in mice (Yao et al., 2007). Furthermore, MGP is differentially expressed during angiogenesis (Albig et al., 2007; Glienke et al., 2000; Javerzat et al., 2009) and is increased in tumor vasculature where it appears to promote tumor angiogenesis in glioblastoma (Kuzontkoski et al., 2010). Finally, MGP deficiency in mice has been shown to cause arteriovenous malformations in lungs and kidneys (Yao et al., 2011). Collectively, MGP has been broadly implicated in angiogenesis and vascular biology but its exact role in this context is unclear. Therefore, the main goal of this study is to investigate a more direct role for MGP during angiogenesis.

Here, we show that MGP suppresses excessive endothelial sprouting, maintains stable vascular luminal structures, prevents excessive microvascular densities, and reduces tumor angiogenesis. Mechanistically, we find that MGP suppresses notch signaling suggesting that MGP may mediate vascular quiescence at least in part by blocking BMP and notch

signaling. Collectively, these results suggest that MGP re-enforces vascular quiescence and promotes angiogenic resolution.

Materials and Methods

Ethics Statement

Animal studies were performed in accordance with the animal protocol procedures approved by the Institutional Animal Care and Use Committee of Indiana State University (protocol #1-19-2008:AA and 11-08-2007:AA).

Mouse Breeding and Genotyping

MGP –/+ mice in C57BL/6 background were generously provided by Gerard Karsenty (Columbia University Medical Center, NY). MGP –/+ mice were crossed with wild type C57BL/6 mice and the siblings were crossed to produce MGP –/– mice. Genotype was determined by PCR amplification of DNA from ear tissue using DirectPCR Lysis Reagent (Viagen Biotech, Inc., LA, CA). PCR was performed using specific primers targeting wild type vs. mutant MGP alleles. The wild type primer pairs targeted a 450 bp wild type MGP allele whereas the mutant primer pairs targeted a 1 Kb MGP mutant allele. Wild type and mutant PCR reactions were performed separately using the following conditions: 1 μl template DNA (from ear sample), 100 nM primers, 1X standard buffer, 320 μM dNTPs, and 66 U/ml Taq polymerase (New England Bio Labs Inc.), and total volume 25 μl. Reactions were cycled according to the following conditions: 94°C for 2 min (1X); [94°C for 45 sec; 57°C for 40 sec; 72°C for 60 sec] (35X); 72°C for 5 min (1X); and 4°C.

Aortic Ring Angiogenesis Assay

Aortas extending from the aortic arch to the diaphragm were removed from five week old C57BL/6 wild type or MGP –/– mice. The aortic sections were washed in 1X PBS and dissected into small rings of equal sizes (~1mm) before implantation into fibrin gels. Fibrin gels were prepared by mixing 1.5 mg/ml fibrinogen with serum free EGM2 media (Lonza Inc.), and filtering through 0.22 μm sterile filters. The fibrin gel was formed by adding 0.06 U/ml Thrombin to 0.5 ml fibrinogen solution in 24-well plates into which the aortic rings was immediately implanted. Fibrin gels were allowed to form at room temperature for 20 minutes before being overlaid with 1 ml EGM2 + growth factors (Lonza Inc.). The plates were incubated in 37 °C in a 5% CO_2 incubator. Aortic rings were observed daily for signs of angiogenic sprouting. Individual sprout lengths were measured after 10 days after brief staining with a 0.2% solution of p-iodo-nitrotetrazolium dissolved in 0.5% ethanol to stain live cells.

MGP morpholino injection in zebrafish

The MGP specific anti-sense morpholino (Genetools) (5′ GAGACACACACATG ACTGCAGGAGC 3′) was designed to interfere with MGP mRNA translation initiation. Morpholinos were dissolved in water and diluted 1:1 into 0.1% phenol red/water injecting solution. 12 ng of MGP morpholino was injected into 1 to 8 cell *Fli1*-GFP/*GATA1*-RFP embryos in a total volume of 0.9 nl per embryo. Embryos were sedated in tricaine and monitored for vascular phenotypes on a Nikon SMZ-1500 fluorescent dissecting microscope. Morpholinos directed against p53 were synthesized and used according to previously published work (Robu et al., 2007).

Immunohistochemistry

Excised tissues were fixed in 4% paraformaldehyde for 1 hr and stored in 70% ethanol before paraffin embedding, sectioning, and staining with CD-31 antibody to visualize

vascular structures in the Clarian Pathology Laboratory at Indiana University (Indianapolis, IN). To quantitate vascular density, CD-31 staining patterns were traced onto white paper with black ink and the resulting copy was scanned to obtain total vascular area using Image J software (NCBI).

Immunobloting

The N-terminally Flag-tagged human MGP (N-Flag-hMGP) plasmid was generously provided by Dr. Kristina Bostrom (UCLA, CA). Approximately, seventy five percent confluent 293T cells in 10 cm plates were transfected with 10 µg of N-Flag-hMGP plasmid DNA using Trans-IT LT1 transfection reagents (Mirus Inc.) as per the manufacturer's recommendations. After 24 hours, plates were washed with 1X PBS and cultured in serum free media (SFM) overnight. Confirmation of MGP expression in the conditioned media was performed by precipitation with .1% DOC/TCA as described in our previous study (Williams et al., 2010) followed by western blot analysis using anti-flag M2-antibody.

RT-PCR

RT-PCR was performed to determine the expression of Delta Like-4 (DLL4), jagged-1, Hes-1, CD31, smooth muscle Actin, MGP, and GAPDH. Total RNA was isolated using Trizol reagents (Life technologies, Grand Island NY) as per the manufacturer's instructions. cDNA was synthesized using the iScript cDNA Synthesis Kit (Bio Rad Inc.). Primer sequences, target genes, and PCR product sizes for each primer set are listed in Table 1. The PCR reactions were performed under the following conditions: 10 ng cDNA; 200 nM oligos; 320 µM dNTP; 1x standard buffer; and 66 U/ml Taq Polymerase in a total reaction volume of 25 µl. Cycling parameters used were as follows: 1 cycle at 94°C for 2 min; 30 cycles at 94°C for 45 sec, 57°C for 40 sec, and 72°C for 60 sec; 1 cycle at 72°C for 5 min; and hold at 4°C.

Transfections and Luciferase Assay

Transient transfection of human microvascular endothelial cells (HMEC) was performed in triplicate in 24-well plates. HMEC cells were seeded into 24-well plates at 20,000 cells/well 20–24 hrs prior to transfection. Individual wells were transfected in triplicate with 200 ng of Hes-1 luciferase plasmid and 25 ng of CMV β-galactosidase control plasmid using Trans-IT LT-1 (Mirus Inc.) reagent according to the manufacturer's recommendations. Two days after transfection, the cells were lysed in 100 µl/well of Passive Lysis Buffer (Promega, Madison, WI), freeze-thawed, and centrifuged for 1 minute. Luminescence activities for luciferase and β-galactosidase were measured by Glomax Luminometer using Promega luciferase assay reagents according to the manufacturer's recommendations.

In-vivo Tumor Growth Studies

Pancreatic Adenocarcinoma (PanO2) cells were resuspended in sterile phosphate buffered saline (PBS) and 1×10^6 cells per 100 µl were injected subcutaneously between the shoulder blades of approximately 10-week-old MGP −/+ and MGP +/+ C57BL/6 mice (three mice per condition; bred in-house). Mice were monitored on a daily basis and primary tumors were measured externally with calipers between days 9 and 17.

Results

MGP suppresses endothelial-sprouting in-vitro

In our previous study, MGP expression was significantly increased during angiogenesis, but the exact role of MGP in this context was not clear (Albig et al., 2007). Here, we used MGP deficient mice to study MGP function during angiogenesis. PCR based genotyping was used

to identify MGP −/− mice and RT-PCR analysis was used to confirm the absence of MGP mRNA in MGP−/− animals (Figure S1). Aortas were isolated from ~ 5 week old MGP +/+ or MGP −/− mice, sectioned, and implanted into fibrin gels. As shown in fig 1A and B, ~ 40% of the MGP −/− rings initiated sprouting on day 3 while MGP +/+ rings did not initiate sprouting until day 4. Furthermore, 100% of the aortic rings from MGP −/− mice had sprouted by day 5 whereas 100% of the MGP +/+ rings only sprouted by day 7. Finally, after ten days in culture, angiogenic sprouts from MGP −/− rings were ~1.5 fold longer compared to angiogenic sprouts from MGP +/+ rings (Fig 1C). To determine if MGP was directly responsible for suppressing aortic sprouting, we generated control or MGP containing conditioned media by transfection of 293T cells (Figure S1) and applied these conditioned medias to MGP+/+ and MGP−/− aortic ring cultures. As shown in figure 1, compared to control conditioned media MGP containing conditioned media delayed sprouting initiation and decreased final sprout length in both MGP+/+ and MGP−/− aortic cultures. Collectively, these results showed that MGP normally acts to suppress angiogenic sprouting and suggested that either 1.) MGP is an endogenous inhibitor of angiogenesis, or 2.) that MGP does not inhibit angiogenesis per se, but rather is important for re-enforcing angiogenic resolution.

MGP suppresses microvascular density in heart and skeletal muscles

Based on the increased sprouting from MGP −/− rings, we predicted that MGP −/− mice might have increased vascular densities compared to MGP +/+ mice. To investigate this, we isolated various tissues from MGP +/+ and MGP −/− mice and used immunohistochemistry with anti-CD31 antibodies to monitor vascular density. Compared to the MGP +/+ mice, MGP −/− mice had significantly increased CD-31 staining in heart (2.8 fold increase) and skeletal muscles (1.7 fold increase) (Fig 2A), suggesting that MGP inhibits formation of excessive microvasculature in these tissues. These results suggested that MGP is crucial in the maintenance of normal vascular densities in skeletal muscle and heart and further emphasized the importance of MGP in microvascular function.

MGP suppresses tumor angiogenesis

In contrast to our results showing that MGP suppresses angiogenic sprouting, MGP was previously shown to promote tumor angiogenesis (Kuzontkoski et al., 2010). These conflicting observations suggested that MGP may have differential roles in normal physiological and pathological angiogenesis and it was therefore important to distinguish between these possibilities. To accomplish this, we subcutaneously injected pancreatic adenocarcinoma (PanO2) cells into syngeneic MGP +/+ or MGP heterozygous (MGP +/−) mice and monitored tumor growth and vascular density in the resulting tumors. Performing this experiment in MGP +/− mice was necessary since MGP −/− mice typically die by five weeks of age, which prohibits long-term tumor studies whereas −/+ mice have normal life spans. As shown in figure 3, tumors grew significantly faster (Fig 3A) and at dissection were approximately 2.5 fold larger in MGP +/− compared to tumors grown in MGP +/+ mice (Fig 3B, C). Immunohistochemistry of tumor sections with anti-CD31 antibodies (Fig 3D, 3E) and RT-PCR analysis of CD31 mRNA (Fig 3F, 3G) revealed that MGP +/− tumors contained approximately 1.5 fold more blood vessels compared to tumors grown in control mice. Therefore, these results are consistent with our previous results and do not support differential roles for MGP in normal vs. pathological angiogenesis.

MGP is important for the maintenance of vascular lumen structures

To further dissect the role of MGP in vascular function, we examined vascular development in zebrafish embryos injected with anti-MGP morpholinos. Multiple sequence alignment of MGP from seven different species including zebrafish indicated that MGP is highly conserved among species (Figure S2) and therefore suggested that MGP is likely to serve

conserved functions in vascular development and function. RT-PCR was used to confirm expression of MGP mRNA in developing zebrafish. As shown in figure S2, MGP mRNA was expressed as early as 10 hours post fertilization (HPF) and continued to be expressed throughout the observed time period. This was consistent with previous observations that showed a similar pattern of MGP expression by immunohistochemistry in zebrafish (Gavaia et al., 2006). Within 24 hours after morpholino injections, MGP morphants showed a progressive developmental defect characterized by an abnormal curvature of the back. A slightly curved phenotype was observed on day 1 (Fig 4A) that became more prominent by day 3 (Fig 4B) and day 6 (Fig 4D). MGP expression in zebrafish has been found in chondrocytes and is important for cartilage mineralization during bone formation (Gavaia et al, 2006). In MGP −/− mice, MGP is important for suppressing pathological calcification of extracellular matrix (Lou et al, 1997). Therefore it is likely that the deformation of MGP morphants is related to the role of MGP in cartilage and bone development. Importantly however, despite the curved phenotype, normal body segmentation was observed (Fig 4A), which is requisite for vascular development (Lawson et al., 2001). Inspection of the vasculature revealed that MGP knockdown slightly delayed the angiogenic sprouting of intersegmental vessels (ISV) from aorta on day one (Fig 4A). However, by day 3 ISV vessels in MGP morphants were similar to those in control fish suggesting MGP is dispensable for the initial establishment of vascular networks. This was consistent with our observations that MGP did not have an observable affect on activities operant during angiogenesis including invasion, proliferation, migration, and tube formation activity of endothelial cells (Figure S3). By day 3 however, MGP-knockdown in the developing zebrafish caused a progressive loss of vascular luminal structures in the ISVs. Day 3 MGP morphants had narrower ISV lumens compared to control fish (Fig 4C, arrows) and blood flow was partially blocked (Fig 4B). By day 6, luminal structures in MGP morphant aortas and ISVs were completely non-evident compared to the control fish (Fig D, E) and MGP morphants developed edema near the anterior side of the heart (Fig 4D, arrow). Overall, these results suggested that MGP is not required for initial vascular development but is crucial for proper maintenance of normal vascular structure.

MGP decreases Notch signaling in cultured endothelial cells

Notch activation by DLL4 and jagged-1 has opposing effects on endothelial sprouting during angiogenesis. Jagged-1 promotes endothelial sprouting and angiogenesis whereas DLL4 suppresses sprouting and promotes vascular quiescence (Benedito et al., 2009). Interestingly, DLL4 knockdown in zebrafish (Leslie et al., 2007), DLL4 −/+ mice (Scehnet et al., 2007), and Dll4 blockade (Noguera-Troise et al, 2006) all exhibit excessive angiogenesis and loss of vascular lumen structures similar to our results with MGP −/− aortic rings and MGP morphants and suggested a link between MGP and notch signaling. To test this, we utilized a notch responsive luciferase construct featuring the Hes-1 promoter upstream of the luciferase gene to examine notch responsive transcription activity in Human Microvascular Endothelial cells (HMEC) cultured in control or MGP conditioned media. MGP containing conditioned media was prepared by transfection of MGP cDNA into 293T cells and expression was confirmed by western blot (Fig S1). Our luciferase data showed that HMECs cultured in MGP conditioned media had decreased Hes-1 activity compared to the control HMECs cultured in control conditioned media (Fig 5A). To support this observation, we performed RT-PCR analysis to determine if MGP controls expression of different components of the notch signaling pathway. To accomplish this, 10 day old aortic ring cultures from MGP +/+ and MGP −/− mice were collected by tryptic digestion of fibrin gels, removal of the original aortic ring, and extractions of RNA from the remaining outgrowths. RT-PCR analysis was performed to compare expression levels of smooth muscle actin (smActin), endothelial cell marker (CD-31), GAPDH, the Notch target gene Hes-1, and the notch ligands jagged-1 and DLL4. RT-PCR detected expression of both

smooth muscle actin (smActin) and CD-31, confirming that aortic outgrowths were co-cultures of smooth muscle and endothelial cells (Fig 5B). More importantly however, expression of jagged-1 mRNA and Hes-1 mRNA in MGP −/− outgrowths was elevated compared to MGP +/+ outgrowths whereas expression of DLL4 mRNA remained unchanged (Fig 5B). Conversely, we also examined gene expression levels in HMEC cells treated with conditioned media collected from control or MGP transfected 293T cells (Fig 5C). Consistent with previous results, MGP significantly decreased expression of jagged-1 and Hes-1 mRNA but did not affect DLL4 mRNA expression. Collectively, this data provided a correlation between MGP function and notch signaling and suggested that MGP might inhibit angiogenic sprouting by suppressing jagged-1 expression.

MGP suppresses aortic sprouting independently of Notch and VEGF signaling

Our results have shown that MGP suppressed angiogenic sprouting and Notch signaling in cultured aortic rings and isolated endothelial cells. Previously, MGP was shown to suppress BMP signaling (Bostrom et al., 2004; Zebboudj et al., 2002). Interestingly, BMP and Notch signaling have been co-implicated in the development of vascular calcification (Shimizu et al., 2011), angiogenic sprouting (Moya et al., 2012) and BMP together with Notch are reported to synergistically suppress VEGF expression (Larrivee et al., 2012; Ricard et al., 2012). Based on these results, it was important to determine if enhanced aortic sprouting in the absence of MGP was a consequence of enhanced Notch, BMP, or VEGF signaling or a synergistic manipulation of these pathways. To address this question, we monitored sprouting from control or MGP −/− aortic rings in the presence or absence of either the BMP antagonist dorsomorphin, the γ-secretase/Notch antagonist DAPT, or the VEGF inhibitor SU5416. As previously shown, MGP −/− aortic sections demonstrated significantly enhanced aortic sprouting compared to aortic rings from control mice (Figure 6A). Surprisingly, inhibition of Notch signaling with DAPT or inhibition of VEGF signaling with SU5416 had a minimal effect on aortic sprouting from both control and MGP knockout aortic rings indicating these signaling mechanisms play a minor role for angiogenic sprouting in this assay. However, inhibition of BMP signaling with dorsomorphin elicited a striking blockade on aortic sprouting from both control and MGP −/− aortic sections suggesting that BMP signaling is the predominant signaling system active under these conditions. Collectively, these results illustrated that MGP does not appear to normally suppress angiogenesis by decreasing Notch or VEGF signaling. Unfortunately, the complete suppression of aortic sprouting in dorsomorphin treated aortic cultures limited our ability to determine if MGP normally suppresses angiogenesis by suppressing BMP signaling.

Discussion

Arteriosclerosis, atherosclerosis, and the inappropriate angiogenesis within tumors collectively account for some of the most common vascular abnormalities of humans. An important realization is that each of these diseases is strongly impacted by interactions between vascular cells and components of ECM in the vascular microenvironment. In light of this, growing interest has been shifted toward understanding the interplay between ECM and endothelial cell activity to dissect the pathophysiology of these vascular diseases.

Matrix Gla protein is an ECM protein commonly found in vascular tissues (Hao et al., 2004; Luo et al., 1997; Yao et al., 2010) and has been implicated in several vascular abnormalities including arteriosclerosis, atherosclerosis, arterial-venous malformations, and abnormal tumor angiogenesis (Kuzontkoski et al., 2010; Luo et al., 1997; Yao et al., 2010; Yao et al., 2011). However, the functional role and mechanistic basis by which MGP impacts these abnormalities is unclear. In this study we used a combination of mice and zebrafish MGP knockout models coupled with cell and tissue culture approaches to refine our understanding of the role of MGP in vascular formation and function.

In order to clarify the role of MGP in angiogenesis, we compared angiogenic sprouting from aortas dissected from wild type or MGP knockout mice. Angiogenesis encompasses both the activation phase wherein vascular networks are established by the proliferation, migration, and invasion of endothelial cells, and the resolution phase wherein vascular networks are stabilized and endothelial cell quiescence is established. Our results show that in the absence of MGP, aortic sprouts appeared significantly earlier and grew to greater lengths compared to control aortic rings (Figure 1). Similarly, Yao et al. showed that MGP suppresses pulmonary blood vessel branching (Yao et al., 2007). This observation suggested that either MGP normally functions to reinforce the resolution phase of angiogenesis or that MGP actively suppresses the activation phase of angiogenesis. Our data does not support the idea that MGP actively suppresses angiogenesis since we were unable to detect any impact of MGP on endothelial cell activities operant during angiogenesis including proliferation, invasion, migration, and capillary formation (Figure S3). Furthermore, our previous findings showed that MGP expression is increased during the later stages of endothelial network formation, consistent with a role during resolution phase (Albig et al., 2007). Finally, ISV sprouting in zebrafish embryos was only minimally impacted by MGP knockdown and the initial establishment of functional vascular networks was normal in MGP morphants (Figure 4B). Therefore, we hypothesize that MGP is important for the establishment and maintenance of the endothelial quiescence program. In support of this hypothesis, CD31 staining of MGP knockout adult tissues revealed increased vascular densities in heart and skeletal muscle, suggesting a failure of vascular tissues to achieve quiescence. In addition, tumors grown in MGP +/− mice contained more blood vessels than their control counterparts further illustrating the role of MGP in vascular development. Finally, the progressive loss of vascular lumens in MGP morphant zebrafish shows that MGP is indispensable for the maintenance of functional vascular lumen structures, an important aspect of quiescent vasculature. Collectively, these data suggest that MGP does not significantly impact angiogenesis activation, but rather is important during the resolution phase of angiogenesis.

In mice, MGP blocks BMP-2/4/7 signaling (Yao et al., 2011; Yao et al., 2006). In the absence of MGP, elevated BMP signaling has been linked to vascular defects including arteriosclerosis, atherosclerosis (Yao et al., 2010), and arterial-venous malformations (Yao et al., 2011). However, in zebrafish embryos, it is not clear that MGP suppresses BMP since zebrafish MGP does not contain a BMP binding domain (Yao et al, 2008). Moreover, the role of BMP signaling in zebrafish intersegmental vessel formation is uncertain since the BMP responsive BRE promoter is not active in developing ISV vessels (Collery and Link, 2011), and specific inhibition of BMP has been shown to have no affect on ISV formation (Cannon et al., 2010) although BMP signaling has been implicated in angiogenic sprouting from the axial vein (Wiley et al., 2011). Taken together, it is not likely that the effect of MGP knockdown on zebrafish ISV luminal structures is strictly due to abnormal BMP signaling. Interestingly, BMP has been shown to function in synergy with Notch signaling (Larrivee et al., 2012; Moya et al., 2012) thus potentially implicating Notch with our results.

Activation of Notch signaling by Jagged-1 or DLL4 initiates opposing angiogenic activities. Although opposing, a balance between Dll4 and Jagged-1 is required to establish and maintain functional vasculature (Benedito et al., 2009). DLL4 promotes quiescent stalk cell selection whereas jagged-1 opposes Dll4 by inducing pro-angiogenic tip cell selection in endothelial cells. Disruption of this balance by Dll4 knockdown in zebrafish drives the initial establishment of functional vasculature followed by excessive angiogenic sprouting and the eventual loss of vascular lumen structures (Leslie et al., 2007). Similarly, blockade of notch ligand DLL4 has been implicated in the development of excessive but non-lumanized vessels in tumors (Li et al., 2007; Noguera-Troise et al., 2006). Similar to these results, we found that MGP morphants experienced a progressive loss of vascular lumen

structures and that MGP−/− aortic rings exhibited excessive angiogenic sprouting compared to their control counterparts. Based on these similarities, we hypothesized that MGP may function via the notch signaling pathway. In support of this hypothesis, our luciferase data revealed that MGP suppressed notch activation in endothelial cells. Moreover, our RT-PCR results from mouse aorta and HMEC cells showed that MGP suppressed Hes-1 and jagged-1 mRNA expression but did not alter DLL4 expression (Figure 5). Therefore, our findings suggested that MGP normally functions to maintain a balance between jagged-1 and DLL4 and that in the absence of MGP, excessive jagged-1 destabilizes stalk cell structures resulting in a failure to achieve a stable, quiescent vasculature. Despite this data, BMP inhibition with dorsomorphin but not Notch inhibition with DAPT completely blocked angiogenic outgrowths from both MGP+/+ and MGP−/− mouse aorta (Figure 6). Therefore, while our *in vitro* gene expression data and zebrafish morpholino data suggest that MGP functions through Notch in these systems, it is not yet clear if BMP, Notch, or an alternative signaling pathway is responsible for the enhanced sprouting observed in MGP −/− aortic ring cultures.

MGP is not only associated with suppression of arteriosclerosis and atherosclerosis, but up-regulation of MGP has also been associated with poor prognosis in breast cancer (Yoshimura et al., 2009), gastric cancer (Guo et al., 2010) and glioblastoma (Kuzontkoski et al., 2010). MGP appears to be significantly up regulated in these cancers and is under evaluation as a potential prognostic marker. In glioblastoma, MGP appears to promote tumor growth, angiogenesis (Kuzontkoski et al., 2010), and migration of glioma cells (Mertsch et al., 2009). In contrast, our findings in pancreatic adenocarcinoma (PanO2) showed that tumors grew more rapidly and were more densely vascularized in MGP+/− mice compared to MGP+/+ mice (Figure 3), suggesting a pleiotropic role for MGP in various cancers. One possibility to explain these conflicting observations involves decreased MGP expression in early stage tumors to enable angiogenesis, and increased MGP expression in larger tumors to promote vascular stabilization and increase tumor perfusion. However, it is evident that additional experimentation is required to more precisely define the role of MGP in tumor growth and angiogenesis.

In summary, we have presented evidence suggesting that MGP promotes angiogenic resolution and vascular stabilization. Our findings provide a new avenue toward understanding the role of MGP in both large as well as small vessel dysfunctions. We believe these results will shed light on the pathogenesis of vascular diseases in which MGP is involved such as tumor angiogenesis, atherosclerosis, arteriosclerosis, and arterial-venous malformation.

Supplementary Material

Refer to Web version on PubMed Central for supplementary material.

Acknowledgments

References

Albig AR, et al. Transcriptome analysis of endothelial cell gene expression induced by growth on matrigel matrices: identification and characterization of MAGP-2 and lumican as novel regulators of angiogenesis. Angiogenesis. 2007; 10:197–216. [PubMed: 17632767]

Benedito R, et al. The notch ligands Dll4 and Jagged1 have opposing effects on angiogenesis. Cell. 2009; 137:1124–35. [PubMed: 19524514]

Bostrom K, et al. Matrix GLA protein stimulates VEGF expression through increased transforming growth factor-beta1 activity in endothelial cells. J Biol Chem. 2004; 279:52904–13. [PubMed: 15456771]

Cannon JE, et al. Intersegmental vessel formation in zebrafish: requirement for VEGF but not BMP signalling revealed by selective and non-selective BMP antagonists. Br J Pharmacol. 2010; 161:140–9. [PubMed: 20718746]

Cao Y. Angiogenesis and lymphangiogenesis in common diseases. Editorial Curr Mol Med. 2009; 9:928.

Carmeliet P. Mechanisms of angiogenesis and arteriogenesis. Nat Med. 2000; 6:389–95. [PubMed: 10742145]

Carmeliet P, Jain RK. Angiogenesis in cancer and other diseases. Nature. 2000; 407:249–57. [PubMed: 11001068]

Collery RF, Link BA. Dynamic smad-mediated BMP signaling revealed through transgenic zebrafish. Dev Dyn. 2011; 240:712–22. [PubMed: 21337469]

Crosier MD, et al. Matrix Gla protein polymorphisms are associated with coronary artery calcification in men. J Nutr Sci Vitaminol (Tokyo). 2009; 55:59–65. [PubMed: 19352064]

Davis GE, Camarillo CW. Regulation of endothelial cell morphogenesis by integrins, mechanical forces, and matrix guidance pathways. Exp Cell Res. 1995; 216:113–23. [PubMed: 7813611]

Davis GE, Senger DR. Endothelial extracellular matrix: biosynthesis, remodeling, and functions during vascular morphogenesis and neovessel stabilization. Circ Res. 2005; 97:1093–107. [PubMed: 16306453]

Dreyfus DC. Angiogenesis - Relationships with Cancer, and Angiogenic Diseases. M S-Medecine Sciences. 1989; 5:516–516.

Folkman J. Angiogenesis-dependent diseases. Semin Oncol. 2001; 28:536–42. [PubMed: 11740806]

Gavaia PJ, et al. Osteocalcin and matrix Gla protein in zebrafish (Danio rerio) and Senegal sole (Solea senegalensis): comparative gene and protein expression during larval development through adulthood. Gene Expr Patterns. 2006; 6:637–52. [PubMed: 16458082]

Glienke J, et al. Differential gene expression by endothelial cells in distinct angiogenic states. Eur J Biochem. 2000; 267:2820–30. [PubMed: 10785405]

Guo L, et al. Discovery and verification of matrix gla protein, a TNM staging and prognosis-related biomarker for gastric cancer. Zhonghua Bing Li Xue Za Zhi. 2010; 39:436–41. [PubMed: 21055170]

Hao H, et al. Expression of matrix Gla protein and osteonectin mRNA by human aortic smooth muscle cells. Cardiovasc Pathol. 2004; 13:195–202. [PubMed: 15210134]

Herrmann SM, et al. Polymorphisms of the human matrix gla protein (MGP) gene, vascular calcification, and myocardial infarction. Arterioscler Thromb Vasc Biol. 2000; 20:2386–93. [PubMed: 11073842]

Ingber DE. Extracellular matrix as a solid-state regulator in angiogenesis: identification of new targets for anti-cancer therapy. Semin Cancer Biol. 1992; 3:57–63. [PubMed: 1378310]

Javerzat S, et al. Correlating global gene regulation to angiogenesis in the developing chick extra-embryonic vascular system. PLoS One. 2009; 4:e7856. [PubMed: 19924294]

Kuzontkoski PM, et al. Inhibitor of DNA binding-4 promotes angiogenesis and growth of glioblastoma multiforme by elevating matrix GLA levels. Oncogene. 2010; 29:3793–802. [PubMed: 20453881]

Larrivee B, et al. ALK1 signaling inhibits angiogenesis by cooperating with the Notch pathway. Dev Cell. 2012; 22:489–500. [PubMed: 22421041]

Lawson ND, et al. Notch signaling is required for arterial-venous differentiation during embryonic vascular development. Development. 2001; 128:3675–83. [PubMed: 11585794]

Leslie JD, et al. Endothelial signalling by the Notch ligand Delta-like 4 restricts angiogenesis. Development. 2007; 134:839–44. [PubMed: 17251261]

Li JL, et al. Delta-like 4 Notch ligand regulates tumor angiogenesis, improves tumor vascular function, and promotes tumor growth in vivo. Cancer Res. 2007; 67:11244–53. [PubMed: 18056450]

Luo G, et al. Spontaneous calcification of arteries and cartilage in mice lacking matrix GLA protein. Nature. 1997; 386:78–81. [PubMed: 9052783]

Mertsch S, et al. Matrix gla protein (MGP): an overexpressed and migration-promoting mesenchymal component in glioblastoma. BMC Cancer. 2009; 9:302. [PubMed: 19712474]

Moya IM, et al. Stalk cell phenotype depends on integration of notch and smad1/5 signaling cascades. Dev Cell. 2012; 22:501–14. [PubMed: 22364862]

Noguera-Troise I, et al. Blockade of Dll4 inhibits tumour growth by promoting non-productive angiogenesis. Nature. 2006; 444:1032–7. [PubMed: 17183313]

Ricard N, et al. BMP9 and BMP10 are critical for postnatal retinal vascular remodeling. Blood. 2012; 119:6162–71. [PubMed: 22566602]

Robu ME, et al. p53 activation by knockdown technologies. PLoS Genet. 2007; 3:e78. [PubMed: 17530925]

Scehnet JS, et al. Inhibition of Dll4-mediated signaling induces proliferation of immature vessels and results in poor tissue perfusion. Blood. 2007; 109:4753–60. [PubMed: 17311993]

Shimizu T, et al. Notch signaling induces osteogenic differentiation and mineralization of vascular smooth muscle cells: role of Msx2 gene induction via Notch-RBP-Jk signaling. Arterioscler Thromb Vasc Biol. 2009; 29:1104–11. [PubMed: 19407244]

Shimizu T, et al. Notch Signaling Pathway Enhances Bone Morphogenetic Protein 2 (BMP2) Responsiveness of Msx2 Gene to Induce Osteogenic Differentiation and Mineralization of Vascular Smooth Muscle Cells. J Biol Chem. 2011; 286:19138–48. [PubMed: 21471203]

Sottile J. Regulation of angiogenesis by extracellular matrix. Biochim Biophys Acta. 2004; 1654:13–22. [PubMed: 14984764]

Stupack DG, Cheresh DA. ECM remodeling regulates angiogenesis: endothelial integrins look for new ligands. Sci STKE. 2002; 2002:PE7. [PubMed: 11842241]

Stupack DG, Cheresh DA. Apoptotic cues from the extracellular matrix: regulators of angiogenesis. Oncogene. 2003; 22:9022–9. [PubMed: 14663480]

Wiley DM, et al. Distinct signalling pathways regulate sprouting angiogenesis from the dorsal aorta and the axial vein. Nat Cell Biol. 2011; 13:686–92. [PubMed: 21572418]

Williams KE, et al. Lumican reduces tumor growth via induction of fas-mediated endothelial cell apoptosis. Cancer Microenviron. 2010; 4:115–26. [PubMed: 21505566]

Yao Y, et al. Inhibition of bone morphogenetic proteins protects against atherosclerosis and vascular calcification. Circ Res. 2010; 107:485–94. [PubMed: 20576934]

Yao Y, et al. Matrix Gla protein deficiency causes arteriovenous malformations in mice. J Clin Invest. 2011; 121:2993–3004. [PubMed: 21765215]

Yao Y, et al. Matrix GLA protein, an inhibitory morphogen in pulmonary vascular development. J Biol Chem. 2007; 282:30131–42. [PubMed: 17670744]

Yao Y, et al. Regulation of bone morphogenetic protein-4 by matrix GLA protein in vascular endothelial cells involves activin-like kinase receptor 1. J Biol Chem. 2006; 281:33921–30. [PubMed: 16950789]

Yoshimura K, et al. Prognostic value of matrix Gla protein in breast cancer. Mol Med Report. 2009; 2:549–53.

Zebboudj AF, et al. Matrix GLA protein, a regulatory protein for bone morphogenetic protein-2. J Biol Chem. 2002; 277:4388–94. [PubMed: 11741887]

Highlights

- We investigate a role for Matrix Gla Protein in angiogenesis resolution.

- We show that MGP suppresses angiogenesis, and promotes vascular quiescence.

- We show that MGP suppresses Notch signaling during angiogenesis.
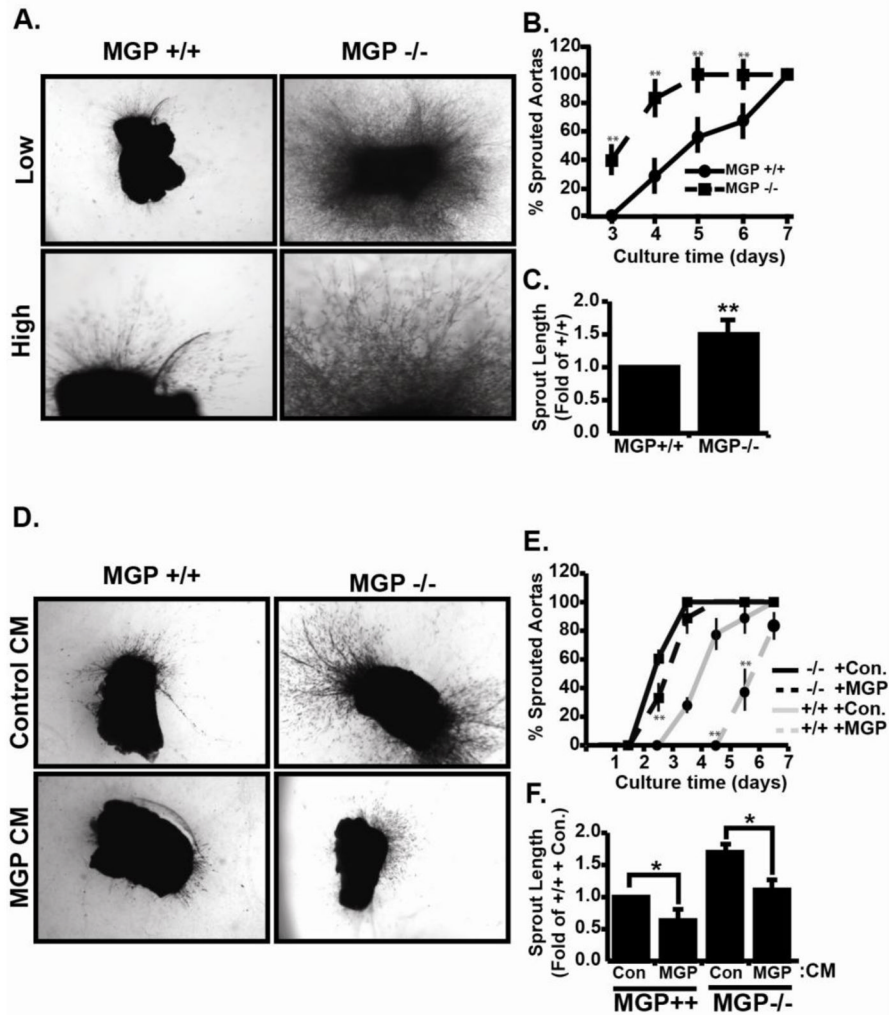
Figure 1. Matrix gla protein (MGP) suppresses endothelial sprouting in mouse aortic rings
(**A**) Aortic rings from MGP +/+ and MGP –/– mice were implanted into fibrin gels, cultured for seven days, and photographed under low and high power magnification. Shown are representative pictures from a single experiment that was performed four times in its entirety. Each experiment consisted of 6–8 aortic ring sections harvested from an individual control or MGP–/– mouse. **B**) The initiation of aortic sprouting was monitored daily and graphed as a percentage of sprouting rings vs time. Data presented are the average +/– SE of four independent experiments. **C**) Average sprout length after seven days in culture was measured using imageJ software. Data represents average +/– SE of four independent experiments. **D**) MGP+/+ and MGP–/– aortic rings were cultured in the presence or absence of control or MGP containing conditioned media collected from 293T cells transfected with MGP cDNA or empty vector sequences. Shown are representative images from a single experiment that was performed three times in its entirety. Each experiment consisted of 3–4 MGP+/+ or MGP–/– rings in control or MGP containing conditioned media. **E**) Sprouting from MGP+/+ and MGP–/– aortic rings in the presence of control or MGP containing conditioned media was monitored daily and the resulting data is depicted as in B. **F**) Average sprout length was measured and the resulting data is presented as in C. In all experiments, * indicates P<.05, student's t-test.
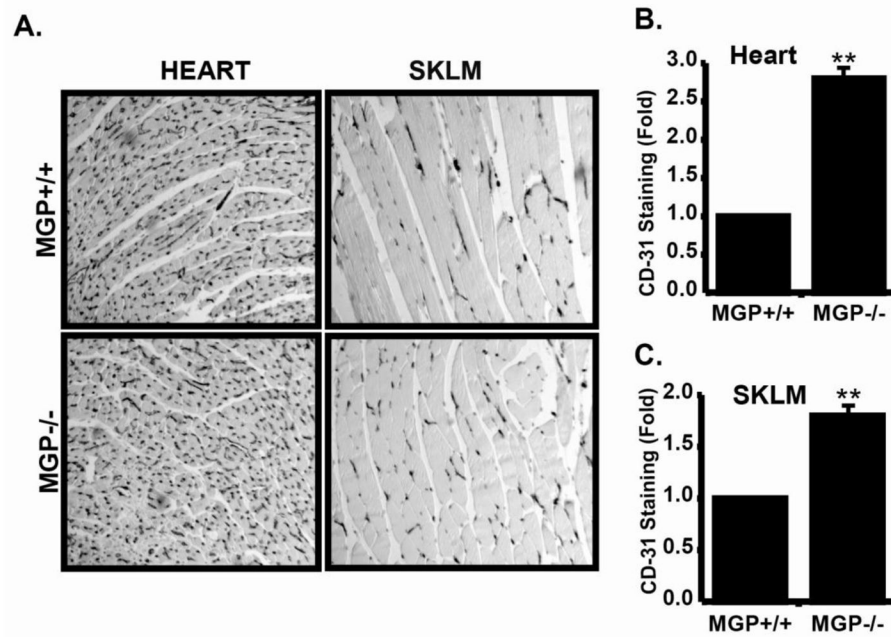
Figure 2. MGP suppresses microvascular density in heart and skeletal muscles
A) Vascular density in heart and skeletal muscle was monitored by immunohistochemistry with anti-CD31 antibodies. Shown are representative images of a single experiment that was performed three times in its entirety. **B**) Quantification of CD-31 staining in heart tissue form MGP +/+ and MGP−/− mice was performed by imageJ analysis. Data shown represents the average +/− SE of three independent experiments and is presented as the fold change compared to MGP+/+ tissue. **C**) CD31 staining in skeletal muscle (SKLM) was quantified and presented as in B. In both B and C, ** Indicates P<0.05, student's-test.
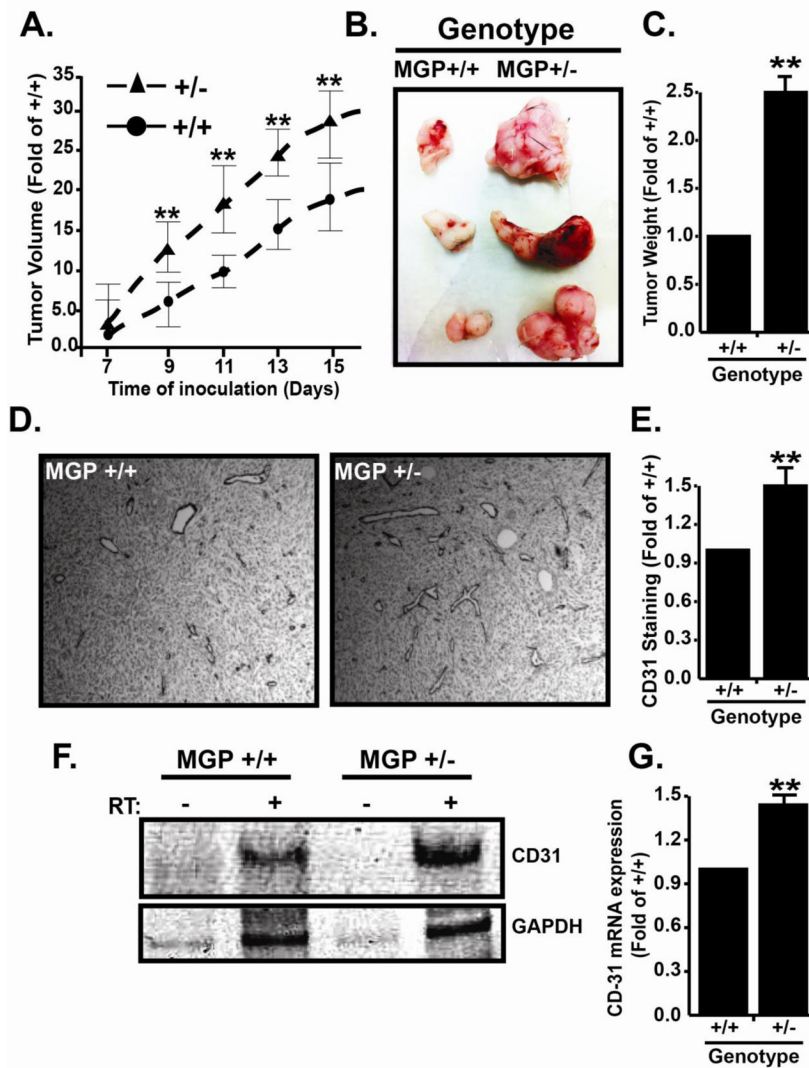
Figure 3. MGP suppresses tumor growth and vascular density

A) Tumor growth was initiated in MGP+/+ or heterozygous (MGP+/−) C57BL/6 mice by subcutaneous injection (in triplicate) of 1×10^6 Pancreatic Adenocarcinoma (PanO$_2$) cells. Tumor sizes were measured one week after injection and subsequently every other day. Data shown depicts average daily tumor size +/− SE compared to tumors grown in control mice. **B**) Representative set of triplicate tumors from a single experiment that was performed three times in its entirety. **C**) Final tumors mass was recorded and is presented as the average fold change (+/−SE) compared to MGP+/+ tumor mass (N=3). **D**) Immunohistochemistry with anti-CD31 antibodies was used to monitor vascular densities in tumors from MGP+/+ and MGP+/− mice. **E**) Anti-CD31 staining in tumors was quantified by imageJ analysis and is presented as the average (+/− SE) compared to MGP+/+ tumors. **F**) Total RNA was extracted from MGP+/+ and MGP+/− tumors and used for RT-PCR analysis of CD31 and GAPDH mRNA expression. Shown are representative images of a single experiment that was performed three times in its entirety. **G**) CD31 RT-PCR results were quantified by imageJ analysis and normalized by GAPDH signal. Data shown depicts CD31 expression in MGP+/− compared to MGP+/+ tumors and is the average (+/− SE) of three independent experiments. In all panels, * indicates P<0.05, Student's t-test.
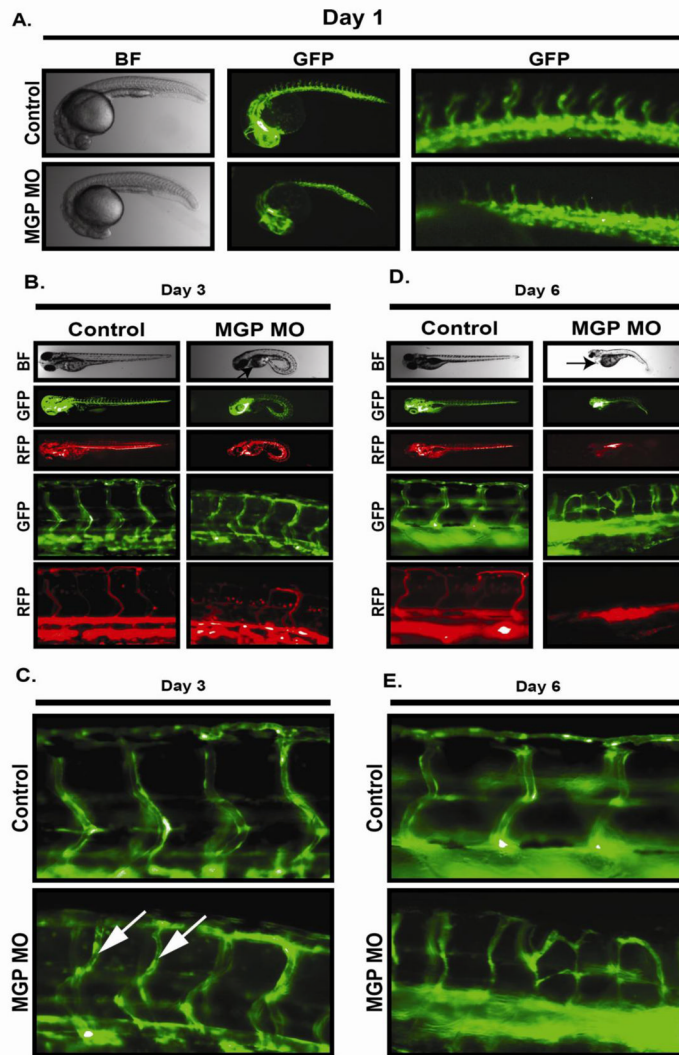
**Figure 4. MGP stabilizes vascular structure in zebrafish embryos**
Fli1-GFP/GATA1-RFP zebrafish embryos between 1 to 8 cells were injected with
morpholino vehicle (water + .1% phenol red) (control) or equal volumes containing 12 ng of
MGP anti-sense Morpholino (MGP MO). **A**) Bright field (BF) and endothelial network
analysis (GFP) of ~24 hour post fertilization (hpf) embryos at low (middle panel) and high
(right panel) magnification. **B**) Analysis of bright field (BF), endothelial network (GFP), and
flow dynamics (RFP) in 3 day post fertilization (dpf) embryos. **C**) High power imaging of
endothelial networks in 3 dpf embryos injected with either vehicle or MGP morpholinos.
Arrows indicate sites of endothelial lumen restriction in MGP morphant. **D**) Analysis of
bright field (BF), endothelial network (GFP), and flow dynamics (RFP) in 6 day post
fertilization (dpf) embryos. Arrow indicates site of edema accumulation in MGP morphant.
E) High power imaging of endothelial networks in 6 dpf embryos injected with either
vehicle or MGP morpholinos.
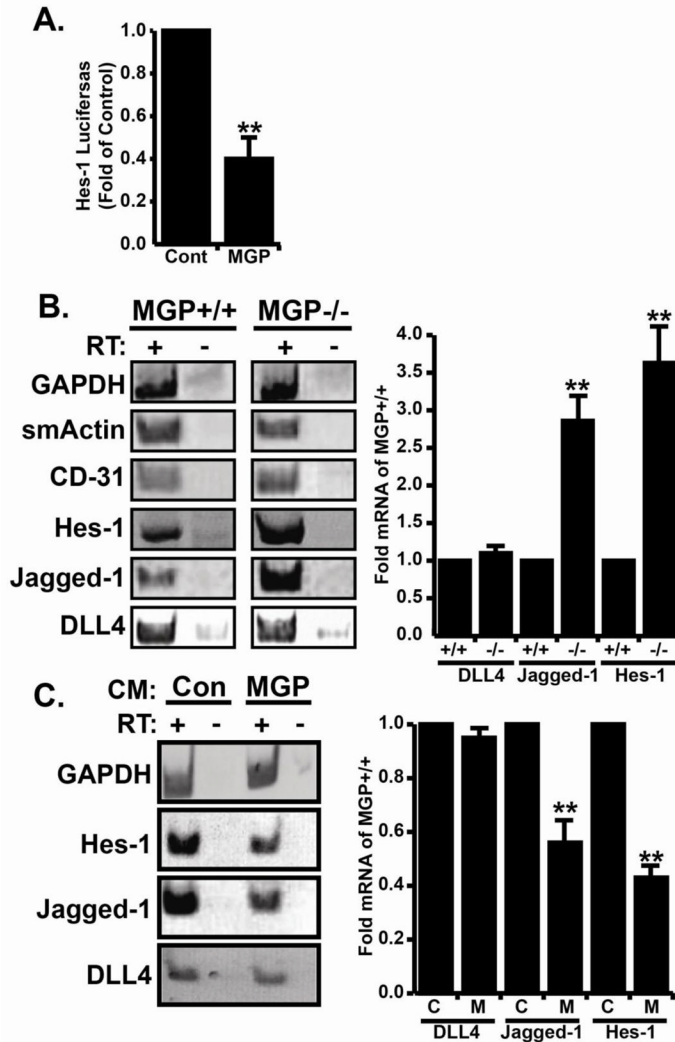
Figure 5. MGP suppresses notch signaling and blocks jagged-1 expression in sprouting endothelial cells

A) Human microvascular endothelial cells (HMECs) were co-transfected with Hes-1 luciferase + CMV-βgal constructs were cultured either with control condition media (Cont) or MGP containing conditioned media (MGP). Data depict the average (+/−SE) of four independent experiments and are presented as the fold change relative to HMEC cells cultured in control conditioned media. **B)** Total RNA was collected from sprouted MGP+/+ or MGP−/− aortic rings and used to perform RT-PCR analysis of smooth muscle actin (smActin), endothelial cell marker (CD-31), GAPDH, Notch target Hes-1, and notch ligands jagged-1 and Delta like 4 (DLL4) genes. Non-reverse transcribed samples were included as a negative control. Shown are representative images of a single experiment that was performed four times in its entirety. ImageJ analysis was used to compare Dll4, Jagged1, and Hes-1 mRNA in MGP+/+ and MGP−/− aortic rings (right panel). Data shown is the average (+/−SE) of four experiments presented as fold change compared to MGP+/+ samples. **C)** Total RNA was collected from HMECs cultured in conditioned media from 293T cells transfected with empty vector (Con), or MGP cDNA (MGP). RT-PCR analysis was to monitor the relative mRNA expression levels of Hes-1, Jagged-1, D114, and GAPDH. Non-reverse transcribed samples were included as a negative control. Shown are representative images from a single experiment that was performed three times in its

entirety. ImageJ analysis was used to compare Dll4, Jagged1, and Hes-1 mRNA in the absence and presence of MGP (right panel). Data shown is the average (+/−SE) of three experiments presented as fold change compared to MGP+/+ samples. In all panels, * indicates P<.05, student's t-test.
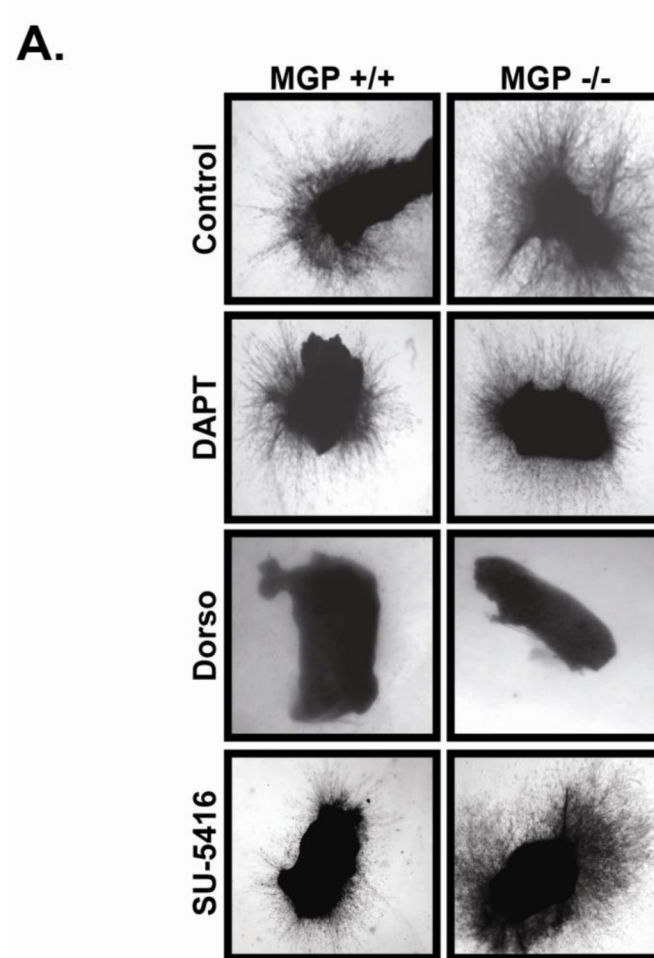
Figure 6. MGP suppresses aortic sprouting independently of Notch and VEGF signaling
Aortic rings were isolated from MGP+/+ or MGP−/− mice and embedded into fibrin gels
containing either vehicle (DMSO), gamma-secretase Notch inhibitor (DAPT), broad
spectrum BMP inhibitor dorsomorphin (Dorso), or VEGFR2 inhibitor (SU5416). Shown are
representative images were collected after 10 days in culture from a single experiment that
was performed three times in it's entirety.

Table 1

List of Oligonucleotides

No.	Oligonucleotide sequences	Targets	Organisms
1.	FORWARDS-5′ GCC ACA ATT TCT GCA TCC TGC 3′ REVERSE- 5′ CGG GAA AGA TGA GGA AGA AGG G 3′	MGP (WT)	Mouse
2.	FORWARD- 5′ TGC CTG AAG TAG CGG TTG TA 3′ REVERSE- 5′ TGA ATG AAC TGC AGG ACG AGG 3′	MGP (Mutant)	Mouse
3.	FORWARD- 5′ GAC AAT GAA TAC GGC TAC AGC AAC 3′ REVERSE- 5′ GTG CAG CGA ACT TTA TTG ATG GTA 3′	GAPDH	Mouse
4.	FORWARD- 5′ TGC TGC AGC TTA TGA CTC TCA GGA 3′ REVERESE- 5′ AAA CAC ACG ACA CGG AGA GAA GTC 3′	MGP	Zebrafish
5.	FORWARD- 5′ AGG CTT CTC ACA AAC GAG GAC ACA 3′ REVERSE- 5′ ATC AAT GAC CAG TTT GCC GCC TTC 3′	GAPDH	Zebrafish
6.	FORWARD- 5′ TCC GTG ACA TCA AGG AGA AGC TGT 3′ REVERSE- 5′ GGA AGC GTT CGT TTC CAA TGG TGA 3′	Aortic smActin	Mouse
7.	FORWARD- 5′ AGC TAG CAA GAA GCA GGA AGG ACA 3′ REVERSE- 5′ TAA GGT GGC GAT GAC CAC TCC AAT 3′	CD-31	Mouse
8.	FORWARD- 5′ TAG TGA ATG TGC CCT GGT GTC CAT 3′ REVERSE- 5′ TGA TCC TAA GGC TGC CAT CAC CAT 3′	Jagged-1	Mouse
9.	FORWARD- 5′ TCT TCC GCA TCT GCC TTA AGC ACT 3′ REVERSE- 5′ GCC AGG TGA AAT TGA GGG GCA ACT 3′	DLL4	Mouse
10.	FORWARDS- 5′ TCC ATG ACA ACT TTG GTA TTC GT 3′ REVERSE- 5′ AGT AGA GGC AGG GAT GAT GTT 3′	GAPDH	Human
11.	FORWARD- 5′ ATT GCC AGC TAC TAC TGC GAC TGT 3′ REVERSE- 5′ TTC TGG CAG GGA TTA GGC TCA CAA 3′	Jagged-1	Human
12.	FORWARD- 5′ CCT GCA TTG TGA ACA CAG CAC CTT 3′ REVERESE- 5′ ACA TGA GCC CAT TCT CCA GGT CAT 3′	DLL4	Human
13.	FORWARD- 5′ TGG AGA AGG CGG ACA TTC TGG AAA 3′ REVERSE- 5′ ATG GCA TTG ATC TGG GTC ATG CAG 3′	Hes-1	Human